ReadMON: A Portable Readout System for the CERN PH-RADMON Sensors

Isidre Mateu, Maurice Glaser, Georgi Gorine, *Student Member, IEEE*, Michael Moll, Giuseppe Pezzullo, and Federico Ravotti, *Member, IEEE*

***Abstract*— PH-RADMON sensors are extensively used for radiation monitoring in the large hadron collider (LHC) experiments. Here, ReadMON, a dedicated and portable readout system for non-LHC applications, is presented. The system is able to source currents up to 32 mA and measure voltages up to 125 V, covering the full operational range of all dosimeters onboard the PH-RADMON sensor. Thus, the total measurement range of the system goes from 0.01 Gy to hundreds of kilogray total ionizing dose, and from few 10^{10} to 10^{15} n_{eq}/cm^2 1-MeV neutron equivalent fluence. Different tests have been carried out at CERN IRRAD facility to prove the system concept and analyze its performance. Errors of only a few percent with respect to the readout done with a commercial source-measuring unit were found.**

***Index Terms*— Dosimetry, radiation monitoring, readout systems.**

I. Introduction

MONITORING of the total ionizing dose (TID) and 1-MeV neutron equivalent fluence (Φeq) is performed at CERN large hadron collider (LHC) experiments using a series of dosimeters integrated on a unique carrier printed circuit board (PCB) known as PH-RADMON sensor [1] (Fig. 1). All the dosimeters show excellent reproducibility and have been calibrated in different radiation environments. As a result of these tests, a set of calibration curves have been defined for each type of device [2]. Depending on the required range and sensitivity of the measurement, the sensor can be equipped with different devices: RadFETs for the TID measurement and silicon p-i-n diodes to monitor Φeq. Tables I and II summarize different dosimeters that will be referred in this paper, together with their main operational characteristics. In the case of RadFETs, the expected radiation fields have been taken into account in choosing the most appropriate devices for CERN applications [1]. If the RadFET is operated under zero bias, the thickness of the gate oxide layer plays a crucial role in the probability of recombination of the generated electron–hole pairs within the oxide and hence in the device response to different linear energy transfer (LET) radiations [3].

Manuscript received September 29, 2017; revised December 1, 2017; accepted December 1, 2017. Date of publication December 18, 2017; date of current version August 15, 2018. This work was supported by the European Union's Horizon 2020 Research and Innovation Program under Grant 654168.

The authors are with the Experimental Physics Department, CERN, CH-1211 Geneva, Switzerland (e-mail: isidre.mateu@cern.ch; maurice.glaser@cern.ch; georgi.gorine@cern.ch; michael.moll@cern.ch; giuseppe.pezzullo@cern.ch; federico.ravotti@cern.ch).

Color versions of one or more of the figures in this paper are available online at http://ieeexplore.ieee.org.

Digital Object Identifier 10.1109/TNS.2017.2784684

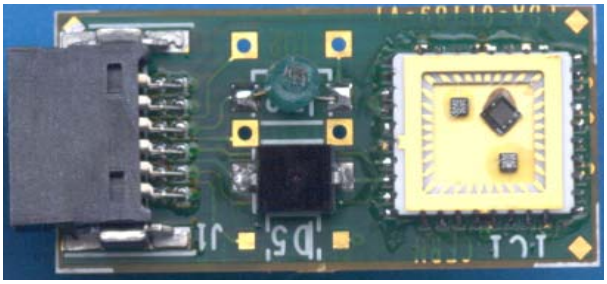

Fig. 1. PH-RADMON sensor consists in a carrier PCB mounting up to 11 devices (RadFETs and/or p-i-n diodes, temperature sensors, and test resistors).

TABLE I
CHARACTERISTICS AND READOUT PARAMETERS FOR THE p-i-n DIODES

	LBSD Si-1	LBSD Si-2	BPW
Fluence range [n_{eq}/cm^2]	$< 10^{12}$	$<2x10^{11}$	$2x10^{12} – 10^{15}$
Sensitivity [$n_{eq}/cm^2/mV$]	$1.6x10^8$	$2.7x10^7$	$9.2x10^9$
Readout current [mA]	25	25	1
Output range [V]	1 – 10	1 – 10	0.5 – 80

TABLE II
CHARACTERISTICS AND READOUT PARAMETERS FOR THE RADFETs

	REM TOT501C 250 nm	LAAS 1600 nm
Dose range [Gy]	$0.1 – 10^5$	<10Gy
Sensitivity [Gy/mV]	0.1	0.01
Readout current [mA]	0.16	0.1
Output range [V]	3.5 – 40	3 – 10

Thus, the Radiation Experiments and Monitors (REM) dosimeters, with thin-gate-oxide layers (130 or 250 nm), show the best response for variable LET radiation, up to doses of 10^5 Gy. On the other hand, to achieve a better sensitivity for doses below 10 Gy, the Laboratory of Analysis and Architecture of Systems (LAAS) dosimeter (with a gate oxide thickness of 1600 nm) has been chosen. In the case of p-i-n diodes, the devices were also selected to cover different

ranges of operation. Provided the readout currents are the ones indicated in Table I, the long base silicon diode (LBSD) sensor is capable of measuring fluence below 10^{12} n_{eq}/cm^2 with a sensitivity of 1.6×10^8 $n_{eq}/cm^2/mV$, while the BPW device can monitor levels up to 10^{15} n_{eq}/cm^2 with a sensitivity of 9.2×10^9 $n_{eq}/cm^2/mV$.

More than 250 PH-RADMON sensors have been installed in the LHC experiments since 2006. In order to fulfill the requirement of integrating the radiation field intensities in various detector control systems (DCS) of the experiments, distributed readout systems, based on specific hardware (often imposed by the DCS architecture chosen by the experiments themselves), are needed for their readout [4]. This results in complex system architectures. Moreover, often, the maximum output value dose or fluence that can be measured with these systems is limited by the maximum rail voltage of the power supply (dimensioned to cope with the radiation expected in the area where the sensor is installed), rather than from the device itself, qualified and calibrated up to higher voltages (e.g., higher radiation levels).

Besides the LHC, PH-RADMON sensors are regularly supplied to other experiments (inside but also outside CERN [5]). In those cases, the users can set up their own readout system or use the sensors in a passive mode, i.e., without active readout [1]. This implies removing it from the experiment and moving it to a laboratory with the appropriate readout equipment. For these applications, a compact and portable readout unit, which could be provided to the users together with the sensors, is of clear interest.

The development of such system, the PH-RADMON reader (ReadMON), is ongoing within the Irradiation Facilities Team in the Experimental Physics Department at CERN [6]. The project is in an advanced phase, with already a consolidated design and a few assembled prototypes. The unit is able to exploit the full range of all the above-mentioned dosimeters, thus featuring a total measurement range from 0.01 Gy to hundreds of kilogray in TID, and from few 10^{10} to 10^{15} n_{eq}/cm^2 in Φ_{eq}. In order to maintain the total uncertainty of the final dosimetry measurement below 15%, we set as a goal that the overall contribution of the readout system to this uncertainty should be lower than 5%. Besides its natural application as a dosimetry reference for high energy physics experiments and/or irradiation facilities, this system could also be of interest in other fields where radiation monitoring is required, such as nuclear [7], industry [8], medical therapy [9], [10] or material testing. Last, but not least, the performance of this full dosimetry system makes it also attractive for possible qualification in space applications.

As a proof of concept, one prototype was tested at CERN IRRAD proton facility [11] in 2016 and another one is currently under test in the GIF++ Gamma Irradiation Facility [12]. Further tests are also ongoing in IRRAD using a more sophisticated test bench, which allows a quantitative assessment of the system performance. The results of the tests carried out in IRRAD, preceded by a general description of the developed ReadMON unit, are presented in this paper.

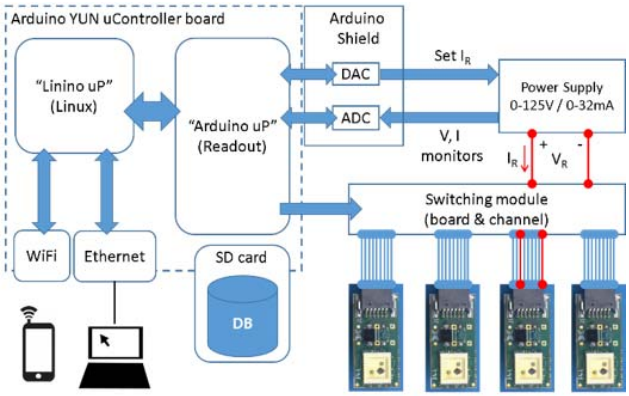

Fig. 2. ReadMON architecture. The system is based on an Arduino YUN microcontroller board with Ethernet and Wi-Fi connectivity. A dc–dc converter provides the readout current dosimeter, and a monitor signal proportional to the readout voltage. A switching module allows selecting the specific dosimeter to be read out from up to eight PH-RADMON sensors.

II. ReadMON Concept

A. Readout Principle

The measurable effect of ionizing radiation in a RadFET is a shift of the transistor gate threshold voltage as a consequence of the buildup of positive charge in the gate oxide [13]. This effect is observable even at zero gate bias of the transistor, thus allowing it to be read out as a two-terminal device. By simply injecting a controlled current, the shift in threshold voltage can be measured. All the RadFET dosimeters qualified for usage in the LHC experiments were calibrated for zero-bias operation.

p-i-n diode dosimeters exploit instead the decrease in conductivity of the intrinsic silicon layer, or base, with increasing particle fluence. This effect is due to the creation of permanent defects in the silicon lattice, which act as recombination centers for minority carriers in the semiconductor [14]. The decrease in conductivity (i.e., increase of resistance) translates into a positive shift of the measured voltage when applying a current pulse in the forward bias direction.

Since both p-i-n diodes and RadFETs share the same readout principle (measurement of the output voltage when injecting a current pulse on a two terminal device), the same current source can be used for the readout of both devices. However, the optimal currents for the readout of every single device as well as the range of measured voltages vary significantly from one device to another, as shown in Tables I and II. These optimal currents are defined, in the case of the RadFETs, as the current at which the thermal effects on the output voltage are minimized; in the case of p-i-n diodes, as the one that maximizes the voltage drop on the diode base, and thus, the sensitivity to resistance changes [1].

B. System Architecture

The ReadMON architecture is shown in Fig. 2. It relies on an Arduino YUN microcontroller board, which includes two microprocessors and is equipped with Ethernet and Wi-Fi interfaces.

The first microprocessor (ATmega32u4) runs the readout sequence by controlling the rest of the ReadMON electronics through the microcontroller input–output terminals. The main element of this electronics is a dc–dc converter (1/8AA12 model from Ultravolt) equipped with a feedback loop enabling it to function as a current source, which is used to supply the readout current to each dosimeter. A 16-bit digital to analog converter is used by the microprocessor to control two input signals of the dc–dc converter: one to set a voltage limit, and the other to select the current to be sourced. Conversely, a 16-bit analog to digital converter (ADC) samples two output signals (monitors) which are proportional, respectively, to the current and voltage supplied by the dc–dc converter. The measurement of the dosimeter output is finally given by this voltage monitor signal.

Dosimeters are read out one at a time, and two multiplexing levels are needed to connect the dc–dc converter output to a specific channel: the first level selects one among eight PH-RADMON sensors, while the second selects one among 11 channels onboard the sensor (the 12th channel being the common ground). A typical RADMON board is equipped with a temperature sensor, a test resistor, and up to nine dosimeters. Thus, in total, the system can address up to 72 single dosimeters, eight test resistors, and eight temperature sensors,

The second microprocessor (Atheros AR9331) runs a Linux distribution in which an application programming interface (API) is implemented. Using simple HTTP requests, the user is able to configure the acquisition settings and retrieve the data, thus allowing the flexibility to integrate the ReadMON in more complex data acquisition systems. For the simplest case of a stand-alone system, a built-in web interface is under development. The data can be stored locally in the secure digital memory card and/or in a remote database.

C. System Capabilities

The exploitation of the full operational range of all PH-RADMON dosimeters (Tables I and II) was the driver for the choice of the dc–dc converter. The chosen unit fulfills the requirement, as it can source a current up to 32 mA, with a voltage limit of 125 V. This broad range in current and voltage makes the ReadMON compatible with other commercially available sensors [15], [16], as well as new ones based on different technologies [17].

The stabilization time is defined here as the time needed for the current delivered by the output of the dc–dc converter to reach a value within 5% of the final voltage after a sudden change of the current setting. The 5% threshold is established in order to keep the total uncertainty of the measurement reasonably low, as explained in Section I.

The stabilization time sets the lower limit for the current pulse duration and is important in the case of p-i-n diodes since keeping these devices under bias too long time during the readout leads to a loss of signal due to self-heating effects [18]. For RadFET devices, the current pulse has to be long enough to minimize the "drift up" of the output voltage [19].

The stabilization time was measured for different load impedances, within the range set by the specifications of each PH-RADMON dosimeter (Fig. 3) and an almost linear dependence was observed. Out of the two p-i-n diodes, the impedance of LBSD device is always below 1 kΩ, so the readout can be done within a few milliseconds. The BPW diode has a maximum impedance of 80 kΩ, still allowing to be read out using a 100-ms-long current pulse. This is short enough to prevent any significant annealing due to self-heating. On the other hand, there is no restriction on the maximum duration of the pulse, so typical current pulses for the readout of the RadFET devices (of the order of a few seconds) can be achieved.

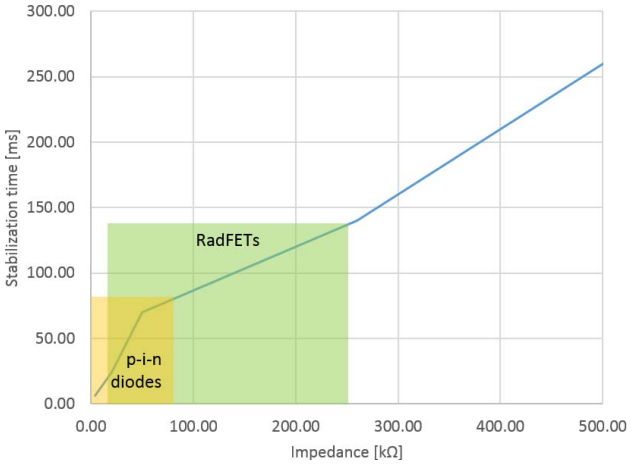

Fig. 3. Stabilization time, as measured for different load impedances. The impedance range of the p-i-n diodes and RadFETs is also represented.

It is worth mentioning that, due to the sequential readout of the dosimeters, the minimum periodicity with which a dosimeter can be read is limited by the amount of dosimeters included in the readout sequence, and the time needed to read out each one of them. The readout time is of the order of 100 ms for the p-i-n diodes, and around 5 s for the RadFETs. Furthermore, some extra 5 s need to be allocated for the readout of the temperature sensor onboard the PH-RADMON (needed to apply corrections on the voltage measurement) and the switching of the relays between measurements. Taking all this into account, in the case of the readout of a single device, the fastest sampling period that can be achieved is, roughly, 5 s for a p-i-n diode and 10 s for a RadFET.

A precise evaluation of the electronic noise for the final product is not possible at this stage, as the final housing and PCB are currently under production. However, as it will be discussed in Section II-D, the data obtained in the different tests show that measurements with an accuracy comparable to that of a commercial source-measuring unit (SMU, Keithley 2410 model) are already possible. Furthermore, although an averaging of multiple voltage measurements over the same current pulse can be configured, this option could not be well exploited for these tests. This is due to the fact that with the current hardware the ADC could be read out only in single-shot mode. In the final version of the circuit, the ADC will be read out in continuous mode, with much faster data rate. (The ADC maximum sampling rate is 860 samples per second.) As a consequence, a higher noise reduction compared to the measurements presented in this paper is expected.

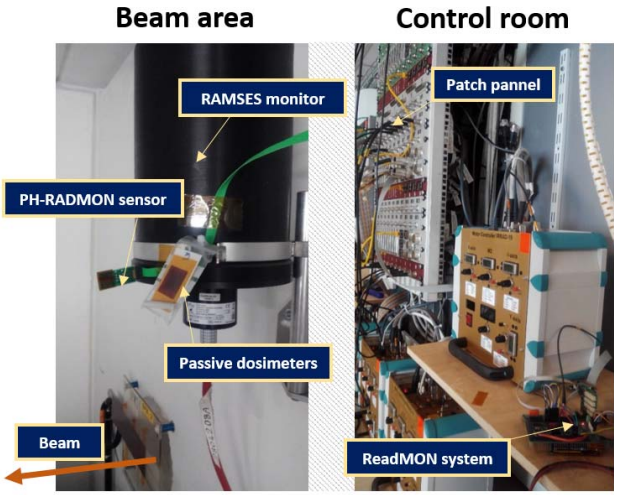

Fig. 4. Setup for the system test in IRRAD. On the left-hand side, the PH-RADMON board installed inside the bunker; on the right-hand side, image of the control room with the readout system connected to the patch panel.

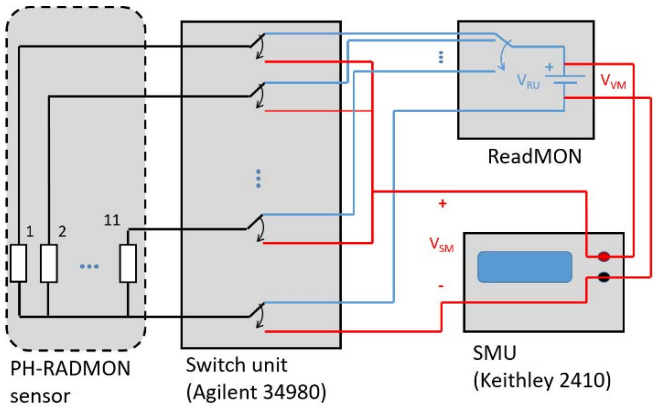

Fig. 5. Schematic view of the test bench installed in IRRAD in 2017. When measuring with the ReadMON, the switch unit is transparent and the dosimeter selection is done internally by the system (blue circuit). The SMU acts in this case as a voltmeter, measuring directly the voltage delivered by the ReadMON. When measuring only with the SMU (red circuit), the switch unit connects it to the dosimeter to be measured.

D. Calibration

The dc–dc converter has been observed to have a certain current offset in the order of some tens of microamperes, which varies from one unit to another. For this reason, it is of utmost importance to properly calibrate the system to ensure that the actual injected current corresponds to the one demanded by the user. This is especially true in the case of the RadFET dosimeters where the optimal readout currents are comparable in magnitude to the offset. In the same way, the voltage measurement provided by the voltage monitor signal of the dc–dc block has to be calibrated against an independent measurement and this is what has been done during the irradiation test in IRRAD in 2017.

III. Irradiation Tests

A. Setup Description

Two different prototype versions were tested in IRRAD in 2016 and 2017. The first test had the main purpose to have a proof of concept of the design, identify and solve potential hardware and software problems, and test the reliability of the system over a long data acquisition run in real conditions. The obtained data were compared with other radiation monitors in order to validate qualitatively the good functioning of the system. The second test, in a more advanced stage of the development, was more ambitious and aimed to validate the readout done by the ReadMON against a benchmark system (commercial SMU).

For the first test, the ReadMON was installed in the control room of the facility and connected through a patch panel to a PH-RADMON sensor inside the beam area (Fig. 4). The sensor was equipped with all the types of dosimeters described in Tables I and II, and was located outside the beam, monitoring the secondary radiation field in the facility to allow for a data acquisition lasting several weeks. (All dosimeters onboard would be saturated within few days if installed directly in the high-intensity 24 GeV/c proton beam.) For this test, the ReadMON was working as a stand-alone system, and was configured to perform a full readout of all the dosimeters every 60 min.

For the 2017 test, a more advanced test bench was installed. Its purpose was to establish a direct comparison between the signal obtained with the ReadMON system and the measurement given by a commercial SMU. A schematic view of the test bench is shown in Fig. 5. In this setup, a switch unit is allowed alternatively connecting the same PH-RADMON sensor to the two readout systems. The test bench was built in such way that, for every readout sequence, the following three different voltage measurements were obtained for the same dosimeter.

1) V_{RU}*:* Measured by the ReadMON at instant t_1 (ReadMON acting as current source).
2) V_{VM}*:* Measured by the SMU at instant t_1 (ReadMON acting as current source).
3) V_{SM}*:* Measured by the SMU at later instant t_2 (SMU acting as current source and ReadMON disconnected).

The data acquisition was configured so that every readout of a dosimeter by the ReadMON was immediately followed by an SMU readout. In this way, the probability of having a proton spill in between the readouts with the two systems was minimized. A LabVIEW interface was used to synchronize all the hardware.

B. Means of Comparison

The data obtained in different tests were compared with other independent measurements obtained either from passive dosimeters installed close to the PH-RADMON sensor under test, or from the secondary emission chamber (SEC) signal. The SEC is a beam instrument located on the irradiation beam line that delivers counts every time a beam pulse (spill) is sent to the facility. The number of pulses is proportional to the number of primary protons in the spill (e.g., the beam intensity). In the case of the passive dosimeters, only a final dose value is extracted at the end of the irradiation, while the

SEC data being logged continuously allow for a comparison during the whole acquisition period.

Different passive dosimeters were used in the tests: Gafchromic film (GaF) [20], radio-photoluminescent glass (RPL) [21], and polymer-alanine detector (PAD) [22]. GaF being a polymer has a higher sensitivity to neutrons, which are the predominant particle in the secondary radiation field of IRRAD, while PAD gives a dose measurement equivalent to that of tissue. The dose measured by the RadFETs is expected to be closer to the one measured by the RPL, which has a material composition and radiation response similar to silicon for highly energetic particles.

C. Calibration Procedure

As it has been discussed in Section II-D, the dc–dc converter needs to be calibrated in terms of injected current and readout voltage. This was not taken into account for the first test in IRRAD, where the interest was centered mainly in demonstrating the working principle of the system. For the second test, the test bench described in Fig. 5 was also used for the calibration of the ReadMON prior to the test. To do so, different resistor values, which covered the range of impedance values of different PH-RADMON dosimeters, were used. The calibration was done in three steps as follow.

1) The SMU was used to accurately measure each resistor value (R).
2) With the ReadMON acting as the current source, a correction curve, V_{VM} versus V_{RU}, was built.
3) The information on the resistor value and the voltage allowed to calculate the real current delivered by the unit and construct a second correction curve for the current setting (I_{set} versus V_{VM}/R).

In both cases, the calibration curves were fit with simple linear equations. In view of the results presented in Sections III-D and III-E, it seems reasonable to explore the possibility of having different calibration parameters depending on the region of operation of the system.

D. Influence of Temperature

The readout of all dosimeters was performed by injecting the current defined in Tables I and II, which minimize the effect of temperature variations on the output voltage. Moreover, the temperature in the IRRAD facility is controlled around 21 °C. Thus, errors due to temperature variations on all acquired data are expected to be negligible.

E. Results

In order to qualitatively assess the correct functioning of the system, the data obtained from the first test in IRRAD in 2016 were compared against the radiation field intensity measured by the SEC.

A very good agreement between the dose and fluence values measured by the ReadMON and the SEC signal trend was found in the ranges of operation of all dosimeters. All the data were converted from voltage to dose or fluence using the calibration curves established in [1]. As an example, the dose

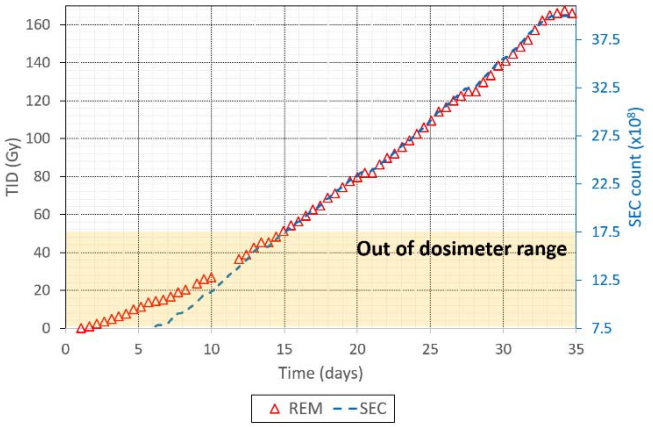

Fig. 6. TID as measured by the REM dosimeter installed in IRRAD (2016) and compared with the SEC signal. The shadowed region is below the operational range of the dosimeter.

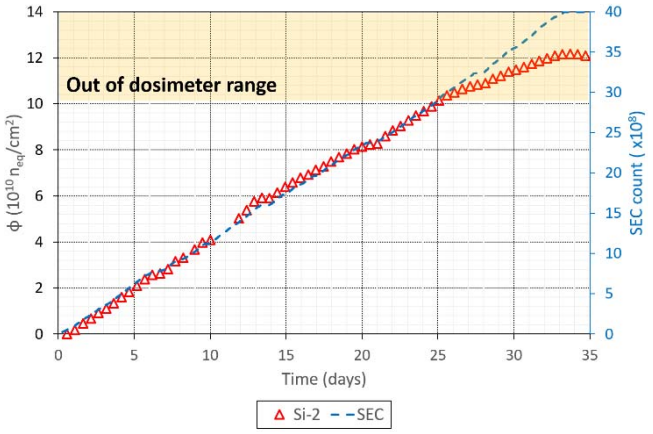

Fig. 7. ϕ_{eq} as measured by the LBSD Si-2 dosimeter installed in IRRAD (2016) and compared with the SEC signal. The shadowed region is above the operational range of the dosimeter.

measured by the REM RadFET is shown in Fig. 6. It can be observed how, up to around 50 Gy, the response of the device is sublinear with respect to the SEC signal, while from this point on there is a perfect overlap between the two signals. This behavior is expected since due to the low dose rate at which the devices are exposed, the competition of the charge buildup with annealing delays the trapping of a measurable quantity of charge and hence the appearance of a significant shift in the transistor threshold voltage. The calibration curve that was used was obtained from accelerated tests with high dose rate [1]. At lower dose rates, such as in the experiment described here, a reduced sensitivity has been observed in the low dose region, which is, therefore, considered as out of the operational range of the device. Fig. 7 shows the example of a very sensitive device (LBSD Si-2 p-i-n diode), which matches perfectly the SEC at the beginning of the irradiation but saturates after a fluence value around 10^{11} n_{eq}/cm^2.

Similar overlaps were obtained for the rest of the dosimeters on the sensor (LBSD Si-1, and BPW p-i-n diode, and a LAAS RadFET). In addition, the dose values obtained at the end of the test from different passive dosimeters, which were

TABLE III
RESULTS OF THE PASSIVE DOSIMETERS INSTALLED IN IRRAD IN 2016

Dosimeter	Dose (Gy)
RPL	205 ± 29
PAD	224 ± 22
GaF	308 ± 15
REM (TID)	170 ± 25

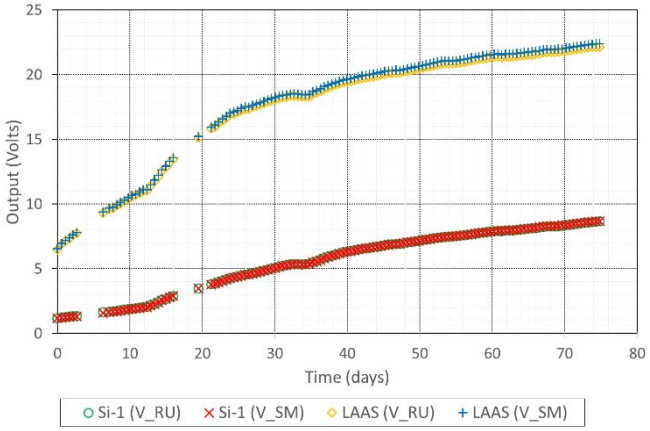

Fig. 8. Comparison of raw voltages obtained with the ReadMON and an SMU, for the LAAS and Si-1 dosimeters onboard the RADMON sensor installed in IRRAD (2017).

exposed together with the PH-RADMON sensor, are summarized in Table III. A reasonably good agreement is found between the final dose measured by the REM RadFET, 170 Gy, and the one obtained from the RPL dosimeter (205 Gy), which, as already discussed, is the one expected to give the closest dose to silicon. The outcome of this test was very encouraging. The working principle of the system was proven, and its reliability over more than one month of data acquisition was verified. Moreover, a basic analysis of the data showed consistent results with respect to the IRRAD beam instrumentation and the passive dosimetry measurements performed in parallel. However, it was still necessary to quantify the accuracy and precision of the readout performed by the system. For this reason, the second setup currently installed in IRRAD allows to benchmark the ReadMON readout with the one performed by an SMU.

Fig. 8 shows the comparison of the raw voltages measured by the ReadMON (V_{RU}) and the SMU (V_{SM}) for a Si-1 p-i-n diode and a LAAS RadFET over around 75 days of acquisition. Similar agreement was observed for the readout of a BPW p-i-n and a REM RadFET, also onboard the sensor. The gaps in the data correspond to interruptions that occurred during the data taking, which were related to problems with the LabVIEW software or to power cuts. There was no data loss due to a malfunctioning of the ReadMON during the whole data taking period.

In order to assess the quality of the voltage calibration carried out before the start of the test, Fig. 9 details the

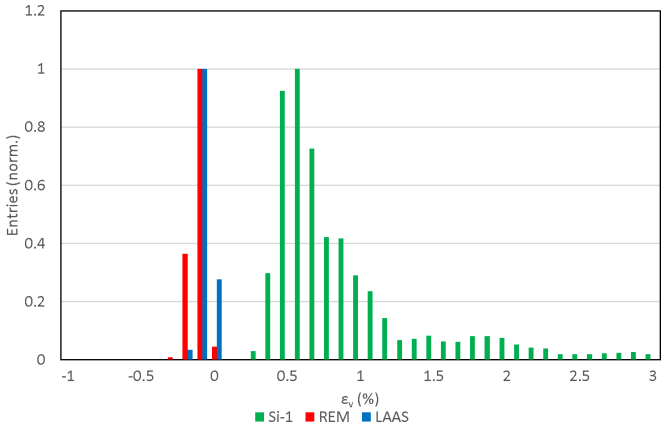

Fig. 9. Voltage error in the measurement given by the ReadMON. The error is calculated with respect to the voltage measured by the SMU acting as a voltmeter.

distribution of the error in the voltage measurement provided by the ReadMON. This error is defined as

$$\varepsilon_V(\%) = \left(\frac{V_{\mathrm{RU}} - V_{\mathrm{VM}}}{V_{\mathrm{VM}}}\right) \times 100$$

where V_{RU} and V_{VM} are the voltage measurements defined.

Three dosimeters are represented in Fig. 9: REM, Si-1, and LAAS. The BPW device is not included since its output voltage changed very little throughout the test. (The measured radiation field intensity was lower than the BPW sensitivity in the measurement location.) For the REM and LAAS, very narrow distributions with close to zero mean (below 0.2%) are observed. For the Si-1 dosimeter, a larger spread in the error appears, with values ranging from 0.3% to 3%. The time evolution of this error revealed that the higher values appeared in the beginning of the irradiation, when the impedance of the Si-1 diode is very low (of the order of ohms). To understand this effect, a careful characterization using low-impedance resistors was carried out, with results showing a loss of linearity of the voltage monitor signal for load impedances below 1 kΩ. This effect will be minimized in the future by using a more refined calibration of the dc–dc converter output.

Finally, in order to evaluate the accuracy of the measurement in terms of dose or fluence, the error on the ReadMON data after conversion to the corresponding units was calculated with respect to the one obtained using the SMU. That is

$$\varepsilon_S(\%) = \left(\frac{S_{\mathrm{RU}} - S_{\mathrm{SM}}}{S_{\mathrm{SM}}}\right) \times 100$$

where S_{RU} refers to the TID or Φ_{eq} obtained with the ReadMON unit and S_{SM} refers to the measurement obtained using the SMU. Fig. 10 shows that the error distributions for all tested dosimeters fall well within the initial 5% goal.

The fact that ε_S is larger than ε_V is to be expected. Indeed, ε_S accounts for different contributions, only one of which is ε_V. Additional sources of error summing up in ε_S are, for example, the statistical fluctuation on the voltage delivered

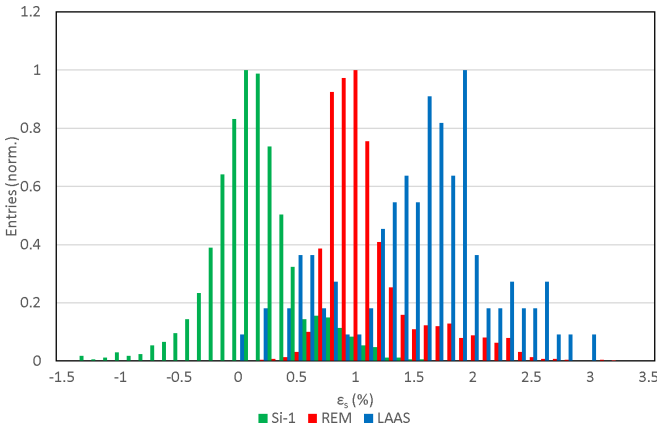

Fig. 10. Dose or fluence error in the measurement given by the ReadMON. The error is calculated with respect to the independent measurement performed by the SMU.

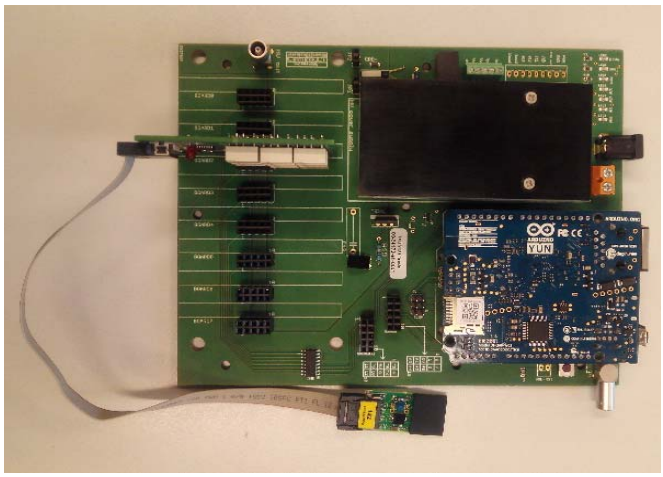

Fig. 11. Most recent prototype of the ReadMON system. All hardware is integrated on the same PCB, which then will be fit in a metal enclosure. Final dimensions of the whole device will be approximately 20 × 15 × 10 cm.

by the sensor, the error on the current delivered by the system, etc.

IV. Conclusion

The development of a new readout system for the PH-RADMON sensors used at CERN and in particular in the LHC experiments has been presented, together with the results of two different tests in IRRAD. Further tests for the validation of the system are ongoing in both IRRAD and GIF++ facilities. The tests done so far have already shown that the system could be used in a real application where online dosimetry measurements are needed. The data obtained with the RADMON reader diverge only slightly from the ones obtained with a high precision commercial SMU.

The aim of this paper is to provide the high-energy physics community, but also other fields where radiation monitoring is a need, with a compact, portable dosimetry system capable of exploiting the full measurement range of the RADMON dosimeters. This will make it a versatile system covering a wide range both in terms of Φ_{eq} (10^{10}–10^{15} n_{eq}/cm^2) and TID (0.1–10^5Gy), with high sensitivity. Moreover, the wide range of current and voltage that can be supplied by the system makes it a suitable candidate for the readout of other sensors beyond the RADMON project. The final system will include a web interface, making it possible to be used as a stand-alone dosimetry measurement device, but will also be provided with an API, thus making it easy to integrate it as a part of more complex data acquisition systems.

All the data presented in this article were obtained during still a development phase of the readout system, with the different prototypes being built reusing old versions of the circuits, interconnected with some modifications built on breadboards. Now a final architecture is consolidated and has been recently implemented in a unique PCB (Fig. 11). This PCB will then be integrated into a metal enclosure to provide shielding from electromagnetic interference. In parallel, the test bench used for the last tests in IRRAD will be further improved adding a direct measurement of the readout current. In addition, the assessment of the system performance at different temperatures, with tests in a climatic chamber, is foreseen. Last but not least, the software part of the project will be further developed in view of arriving to a final product ready to be exploited by the users.

Acknowledgment

The authors would like to thank M. Uğur Kılıç from METU, Ankara, Turkey, for his contribution to this paper, and the colleagues of the IRRAD Team, CERN, Geneva, Switzerland. for reviewing this paper.

References

[1] F. Ravotti, "Development and characterisation of radiation monitoring sensors for the high energy physics experiments of the CERN LHC accelerator," Ph.D. dissertation, Dept. Electron., Univ. Montpellier II, Montpellier, France, 2006.

[2] F. Ravotti, M. Glaser, and M. Moll. (2005). Sensor catalogue data compilation of solid-state sensors for radiation monitoring. CERN, Geneva, Switzerland. [Online]. Available: http://cdsweb.cern.ch/record/835408

[3] R. L. Pease, M. Simons, and P. Marshall, "Comparison of pMOSFET total dose response for Co-60 gammas and high-energy protons," *IEEE Trans. Nucl. Sci.*, vol. 48, no. 3, pp. 908–912, Jun. 2001, doi: 10.1109/23.940131.

[4] F. Ravotti *et al.* (2005). TOTEM on-line radiation monitoring system. CERN, Geneva, Switzerland. [Online]. Available: https://edms.cern.ch/document/874945

[5] C. Aidala *et al.*, "The PHENIX forward silicon vertex detector," *Nucl. Instrum. Methods Phys. Res. A, Accel. Spectrom. Detect. Assoc. Equip.*, vol. 755, pp. 44–61, Aug. 2014. [Online]. Available: https://doi.org/10.1016/j.nima.2014.04.017

[6] *CERN Irradiation Facilities*. Accessed: Sep. 28, 2017. [Online]. Available: https://ep-dep-dt.web.cern.ch/irradiation-facilities

[7] B. Camanzi and A. G. Holmes-Siedle, "The measurement of ultra-high radiation environments: Accelerators and nuclear fusion reactors," presented at the RADECS, 2006.

[8] R. Edgecock, "Industrial application of accelerators," STFC-Rutherford Appleton Lab., Oxfordshire, U.K., Tech. Rep., 2016. [Online]. Available: https://indico.cern.ch/event/569698/

[9] A. B. Rosenfeld, "Electronic dosimetry in radiation therapy," *Radiat. Meas.*, vol. 41, pp. S134–S153, Dec. 2006.

[10] V. Gracanin *et al.*, "A convenient verification method of the entrance photo-neutron dose for an 18 MV medical linac using silicon p-i-n diodes," *Radiat. Meas.*, vol. 106, pp. 391–398, Nov. 2017.

[11] F. Ravotti, B. Gkotse, M. Moll, and M. Glaser, "IRRAD: The new 24GeV/c proton irradiation facility at CERN," in *Proc. AccApp*, Washington, DC, USA, 2015, pp. 182–187. [Online]. Available: http://accapp15.org/wp-content/data/index.html

[12] D. Pfeiffer *et al.*, "The radiation field in the Gamma Irradiation Facility GIF++ at CERN," *Nucl. Instrum. Methods Phys. Res. A, Accel. Spectrom. Detect. Assoc. Equip.*, vol. 866, pp. 91–103, Sep. 2017. [Online]. Available: https://arxiv.org/abs/1611.00299

[13] A. Holmes-Siedle and L. Adams, *Handbook of Radiation Effects*. Oxford, U.K.: Oxford Science Publications, 2002.

[14] J. M. Swartz and M. O. Thurston, "Analysis of the effect of fast-neutron bombardment on the current-voltage characteristic of a conductivity-modulated $p-i-n$ diode," *J. Appl. Phys.*, vol. 37, no. 2, pp. 745–755, Jan. 1966.

[15] M. S. Andjelković, G. S. Ristić, and A. B. Jakšić, "Using RADFET for the real-time measurement of gamma radiation dose rate," *Meas. Sci. Technol.*, vol. 26, no. 2, p. 025004, 2015, doi: 10.1088/0957-0233/26/2/025004.

[16] REM Oxford Ltd., Oxford, United Kingdom. *REM Data Sheet—RFTDAT-CC10—Rev W*. Accessed: Sep. 28, 2017. [Online]. Available: http://www.ee.nmt.edu/~anders/courses/ee521s12/radfet_datasheet.pdf

[17] G. Gorine *et al.*, "Ultra high fluence radiation monitoring technologies for the future circular collider at CERN," presented at the RADECS, 2017.

[18] V. Nagarkar, G. Entine, P. Stoppel, L. Cirignano, and P. Swinehart, "Solid state neutron dosimeter for space applications," *IEEE Trans. Nucl. Sci.*, vol. 39, no. 4, pp. 966–970, Aug. 1992.

[19] A. G. Holmes-Siedle and L. Adams, "The mechanisms of small instabilities in irradiated MOS transistors," *IEEE Trans. Nucl. Sci.*, vol. NS-30, no. 6, pp. 4135–4140, Dec. 1983.

[20] Ashland Advanced Materials, Bridgewater, NJ, USA. *Gafchromic Radiochromic Dosimetric Films by Ashland Advanced Materials*. Accessed: Sep. 28, 2017. [Online]. Available: http://www.gafchromic.com

[21] F. Coninckx, H. Schönbacher, M. Tavlet, G. Paic, and D. Razem, "Comparison of high-dose dosimetry systems for radiation damage studies in collider detectors and accelerators," *Nucl. Instrum. Methods Phys. Res. B, Beam Interact. Mater. At.*, vol. 83, pp. 181–188, Oct. 1993.

[22] M. P. R. Waligórski, G. Danialy, K. S. Loh, and R. Katz, "The response of the alanine detector after charged-particle and neutron irradiations," *Appl. J. Radiat. Appl. Instrum. A, Appl. Radiat. Isotopes*, vol. 40, nos. 10–12, pp. 923–933, 1989.